ChemComm

This article is part of the

# Mechanochemistry: fundamentals and applications in synthesis

web themed issue

Guest editors: Stuart James and Tomislav Friščić

All articles in this issue will be gathered together online at
www.rsc.org/mechanochemistry

ChemComm

RSC Publishing

COMMUNICATION

# Facile synthesis and regeneration of $Mg(BH_4)_2$ by high energy reactive ball milling of $MgB_2$†

Cite this: *Chem. Commun.*, 2013, **49**, 828

Received 10th September 2012, Accepted 3rd December 2012

DOI: 10.1039/c2cc36580d

www.rsc.org/chemcomm

Shalabh Gupta,[a] Ihor Z. Hlova,[ab] Takeshi Kobayashi,[a] Roman V. Denys,[c] Fu Chen,[a] Ihor Y. Zavaliy,[c] Marek Pruski*[ad] and Vitalij K. Pecharsky*[ab]



**We report direct hydrogenation of $MgB_2$ in a planetary ball mill. Magnesium borohydride, $Mg(BH_4)_2$, and various polyhedral borane anion salts have been synthesized at pressures between 50 and 350 bar $H_2$ without the need for subsequent isothermal hydrogenation at elevated temperature and pressure. The obtained products release ~4 wt% $H_2$ below 390 °C, and a major portion of $Mg(BH_4)_2$ transforms back to $MgB_2$ at around 300 °C, demonstrating the possibility of reversible hydrogen storage in an $Mg(BH_4)_2$–$MgB_2$ system.**

Light metal borohydrides, $M(BH_4)_n$ (M = Li, Mg, Ca; *n* is the valence of M), are promising materials for hydrogen storage.[1,2] In particular, $Mg(BH_4)_2$ has been broadly studied because of its favourable enthalpy of dehydrogenation.[3,4] Complete dehydrogenation yields 14.8 wt% of $H_2$ *via* multiple competing processes, ultimately leading to the formation of $MgB_2$.[5] Thus, hydrogenation of $MgB_2$ at reasonably low hydrogen pressure is of great interest. Partial hydrogenation of $MgB_2$ was achieved in two recent studies by coupling mechanochemical processing with subsequent isothermal hydrogenation at high temperature and pressure. Severa *et al.* achieved ~75% yield of β-$Mg(BH_4)_2$ by heating ball-milled $MgB_2$ to 400 °C under 950 bar $H_2$ for 104 h.[6] Li *et al.* reported 25% yield of $Mg(BH_4)_2$ by milling $MgB_2$ under 10 bar $H_2$ for 10 h followed by isothermal hydrogenation at 400 °C and 400 bar $H_2$ for 24 h.[7] Here, we examine the hydrogenation of $MgB_2$ solely by mechanochemical processing[8a–c] under high-pressure hydrogen at room temperature, and study (de)hydrogenation pathways using temperature-programmed desorption (TPD) and solid-state (SS) NMR spectroscopy.

$MgB_2$ (Alfa Aesar, 99% purity) was hydrogenated in a planetary ball mill (Fritsch P-7) using different milling times $\tau_{BM}$ at constant $H_2$ pressure, $p_H$ = 350 bar, or different $p_H$ at constant $\tau_{BM}$ = 15 h. The thermal dehydrogenation was studied by TPD with 5 °C $min^{-1}$ ramping up to 390 °C using an automated Sievert's type PCT (pressure–composition–temperature) instrument (PCTPro-2000, Hy-Energy LLC). All manipulations were performed under an Ar atmosphere in a glove box. Additional experimental details have been reported elsewhere.[9]

Noting that not all of the hydrogen adsorbed during the ball milling is necessarily released below 390 °C, for $\tau_{BM} \leq 15$ h the amount of desorbed hydrogen increases linearly up to 3.1 wt%, reaching a plateau of 3.9 wt% of $H_2$ at $\tau_{BM} \approx 45$ h (Fig. 1a). Similarly, hydrogen desorption increases with $p_H$, before levelling off at 3.2 wt% for $p_H$ = 300 bar (Fig. 1b). Fig. 1c shows the transient of hydrogen desorption from the sample ball-milled under 350 bar $H_2$ for 15 h. The curve indicates two-step dehydrogenation, with peaks observed at 300 and 355 °C. The subsequent SSNMR experiments provided further insight into the hydrogenation and dehydrogenation pathways.

Fig. 2 shows the $^{11}B$ direct polarization magic-angle spinning (DPMAS) spectra of the hydrogenated products, measured using a small flip angle (<15°).[10,11] All spectra consist largely of two manifolds of spinning sidebands, with isotropic peaks (centerbands) located at about 98 ppm and −39 ppm. These were assigned to

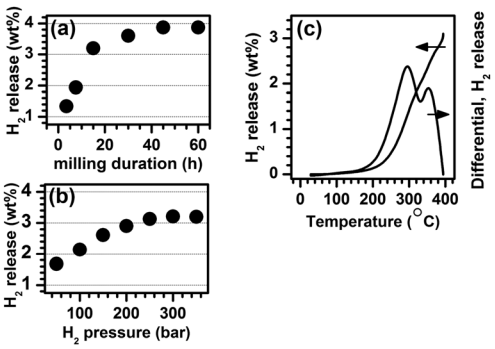


**Fig. 1** Thermal dehydrogenation of mechanochemically hydrogenated $MgB_2$ measured by TPD. (a) $H_2$ desorption from samples hydrogenated for variable $\tau_{BM}$ ($p_H$ = 350 bar). (b) $H_2$ desorption from samples ball-milled at variable $p_H$ ($\tau_{BM}$ = 15 h). (c) $H_2$ desorption curves for the sample ball-milled at $p_H$ = 350 bar for 15 h (ball-to-sample mass ratio B/S = 160).

[a] *Ames Laboratory, Iowa State University, Ames, IA 50011, USA*
[b] *Department of Materials Science and Engineering, Iowa State University, Ames, IA 50011, USA. E-mail: vitkp@ameslab.gov*
[c] *Physico-Mechanical Institute NAS Ukraine, 5 Naukova Str., 79601 Lviv, Ukraine*
[d] *Department of Chemistry, Iowa State University, Ames, IA 50011, USA. E-mail: mpruski@iastate.edu*

† Electronic supplementary information (ESI) available: Detailed experimental conditions, tables of $H_2$ released (in wt%) during TPD, XRD analysis of ball-milled samples, and $^{11}B$ NMR spectra of references. See DOI: 10.1039/c2cc36580d

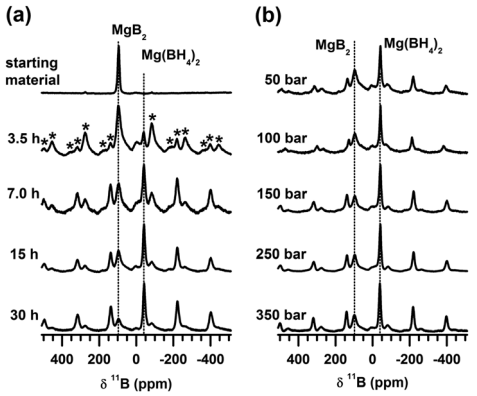


**Fig. 2** Hydrogenation: $^{11}$B DPMAS spectra of $MgB_2$ hydrogenated in the ball mill using (a) $p_H$ = 350 bar, $\tau_{BM}$ = 3.5, 7, 15 and 30 h; and (b) $\tau_{BM}$ = 15 h, $p_H$ = 50, 100, 150, 250 and 350 bar. B/S = 160. Asterisks represent spinning sidebands. The spectra are normalized to constant height.

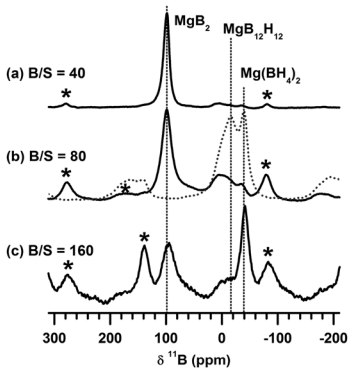


**Fig. 3** Hydrogenation: $^{11}$B DPMAS (solid) and CPMAS (dotted) spectra (normalized to constant height) of samples ball-milled at $p_H$ = 350 bar, $\tau_{BM}$ = 7 h and various B/S ratios. Asterisks represent spinning sidebands. The CPMAS spectrum features only those $^{11}$B nuclei that strongly interact with hydrogen (a subset of all nuclei detected by DPMAS).

$MgB_2$ and $Mg(BH_4)_2$, respectively, based on the spectra of reference compounds (see ESI†).

Quantitative $^{11}$B NMR measurements are challenging due to the complex nutation behaviour of quadrupolar nuclei (for $^{11}$B, $I$ = 3/2) following rf-pulse excitation.[10] In this case, an added difficulty is apparent, since the observed manifolds of spinning sidebands do not originate from the typically encountered quadrupolar or chemical shift anisotropies, but stem mainly from the broadening due to bulk magnetic susceptibility (BMS). The large BMS in the hydrogenated products is due to ferromagnetic impurity (metallic bcc Fe from the milling medium[8b]) as substantiated by SEM-EDX (scanning electron microscopy–energy dispersive X-ray spectroscopy) analysis and the attraction of the samples to the magnet. The resulting local magnetic fields are of dipolar form and are responsible for the observed effects.[12,13] Despite these complexities, one may assume that in each sample the widths of BMS-induced sideband patterns are similar for all peaks, and simply use the centerband intensities to estimate the relative concentrations of species. From SEM-EDX analysis, 10–15 wt% Fe impurity is present in the sample with $\tau_{BM}$ = 60 h. We note that Fe is not incorporated in the $MgB_2$ (Fig. S1, ESI†), nor does it form a mixed-metal hydride phase as would be evident from the NMR peak shifts compared to pure $Mg(BH_4)_2$. Fe impurities do not absorb hydrogen resulting in a gravimetric penalty. Hence, the concentration of hydrogen shown in Fig. 1a may be underestimated for this sample by 12–18%.

The SSNMR spectra confirm the results of PCT analysis. The $Mg(BH_4)_2$ signals are clearly seen at $\tau_{BM} \geq$ 3.5 h (Fig. 2a) and $p_H \geq$ 50 bar (Fig. 2b), and they increase concurrently with the decline of $MgB_2$. The relative signal intensity of $Mg(BH_4)_2$ is consistent with the amount of hydrogen desorbed as shown in Fig. 1a and b. In addition, a broad signal is observed at around −4 ppm, providing a clue to the reaction pathways involved.

Fig. 3 shows the $^{11}$B DPMAS spectra of samples processed at various ball-to-sample mass ratios (B/S). Larger B/S ratios (*i.e.* higher milling energies) increase the $Mg(BH_4)_2$ yield. These spectra also provide information about the hydrogenation reaction pathways. First, when B/S = 40 and 80, the broad signal centred at −4 ppm is stronger than that of $Mg(BH_4)_2$. Second, this signal declines with increasing milling time. Third, it is also present in the $^{11}$B{$^1$H} cross-polarization (CP) MAS spectrum, which confirms that the corresponding $^{11}$B nuclei interact strongly with protons. Finally, the centre of gravity of this signal is at a lower frequency (around −15 ppm) in the CPMAS spectrum than in the DPMAS spectrum. These findings suggest that the broad signal results from the ensemble of various complex anion intermediates, described as $[B_xH_y]^{n-}$ ($n$ = 1, 2).[5,14,15] In particular, the large contribution at −15 ppm in the CPMAS spectrum when B/S = 80 can be assigned to $[B_{12}H_{12}]^{2-}$ species.[5]

$MgB_2$ has the hexagonal graphite-like structure of boron sheets separated by closely packed layers of Mg atoms.[16] High-energy ball milling breaks down the $MgB_2$ structure, generating dislocations, defects, and new grain-boundaries, thus forming trapping sites for hydrogen, and creates dangling bonds, leading to the formation of B–H and Mg–H bonds, polyhedral borane anion intermediates, and, ultimately, $Mg(BH_4)_2$ as the final product. The formation of polyhedral borane anions suggests that some of the B–B bonds present in $MgB_2$ are retained, and new (undesirable) B–B bonds are created as well. Theoretical study of the hydrogenation of $MgB_2$ suggests that hydrogen is present on the $MgB_2$ surface in an atomic form due to low activation energy for dissociation.[17] Thus, higher $p_H$ increases the concentration of atomic hydrogen on the $MgB_2$ surface, favouring the formation of B–H bonds over the B–B bonds. The retention and regeneration of B–B bonds lead to stable polyhedral borane salts, and therefore, reduce the efficiency of mechanochemical formation of $Mg(BH_4)_2$. In earlier studies, mechanochemical processing alone was insufficient to hydrogenate $MgB_2$, and additional isothermal hydrogenation at high pressure was required.[7,18] Nevertheless, the product contained a significant amount of $MgB_{12}H_{12}$. The high intensity of mechanical energy used here together with moderately high $p_H$ leads to a more efficient cleaving of the B–B bonds under milder conditions (temperature and $\tau_{BM}$).

In the following, we scrutinize the thermal dehydrogenation and subsequent rehydrogenation of a sample hydrogenated at $p_H$ = 350 bar, $\tau_{BM}$ = 15 h and B/S = 160. After dehydrogenation at 300 °C, the sample shows a significantly increased concentration of $MgB_2$ and a diminished peak due to $Mg(BH_4)_2$, accompanied by the resonance previously ascribed to $[B_xH_y]^{n-}$ anions (including $[B_{12}H_{12}]^{2-}$) (compare Fig 2a and 4a).[14] Further treatment at 390 °C

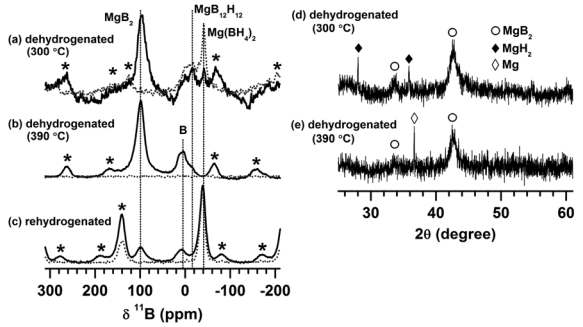


**Fig. 4** Dehydrogenation and subsequent rehydrogenation: (a–c) $^{11}$B DPMAS (solid) and CPMAS (dotted) spectra and XRD patterns of samples (a, d) dehydrogenated at 300 °C, (b, e) dehydrogenated at 390 °C, and (c) rehydrogenated. The hydrogenation and rehydrogenation were carried out at room temperature using $p_H$ = 350 bar, $\tau_{BM}$ = 15 h and B/S = 160. Asterisks represent spinning sidebands. The heights of spectra were adjusted for visual clarity.

results in a complete conversion of $Mg(BH_4)_2$ to dehydrogenated products (as evidenced by the lack of $^{11}B\{^1H\}$ CPMAS signal in Fig. 4b), with $MgB_2$ being the main product. The minor signal centred at 6 ppm in Fig. 4b is characteristic of amorphous boron.[19] Also, in addition to $MgB_2$, the powder X-ray diffraction (XRD) analyses reveal the formation of $MgH_2$ and Mg in the samples dehydrogenated at 300 and 390 °C, respectively (Fig. 4d and e). These results suggest the following dehydrogenation pathways in $Mg(BH_4)_2$ synthesized by reactive ball milling:

$$Mg(BH_4)_2 \rightarrow MgB_2 + 4H_2 \quad (1)$$

$$Mg(BH_4)_2 \rightarrow 1/6MgB_{12}H_{12} + 5/6MgH_2 + 13/6H_2 \quad (2a)$$

$$MgB_{12}H_{12} \rightarrow Mg\ (MgH_2) + 12B + 6H_2\ (5H_2) \quad (2b)$$

$$MgH_2 \rightarrow Mg + H_2 \quad (2c)$$

Note that in addition to $MgB_{12}H_{12}$, other $[B_xH_y]^{n-}$ species are also possible in the sample dehydrogenated at 300 °C. The hydrogen desorption at around 300 °C (Fig. 1c) is attributed to eqn (1) and (2a), while the desorption at around 355 °C is described by eqn (2b) and (2c). An earlier report described multi-step thermal dehydrogenation of crystalline $Mg(BH_4)_2$; $Mg(BH_4)_2 \rightarrow MgH_2 + [B_xH_y]^{n-} + H_2$ (between 280 and 350 °C) and $MgH_2 \rightarrow Mg + H_2$ (~410 °C).[5] In that study, the formation of $MgB_2$ was only observed after heating to 550 °C. In contrast, $MgB_2$ forms already at 300 °C in the present study, whereas $MgH_2$ and Mg form at temperatures similar to those reported in ref. 5 (Fig. 4d and e). These results imply the feasibility of a direct pathway from $Mg(BH_4)_2$ to $MgB_2$ without the formation of stable intermediates (eqn (1)), which is likely related to both the nanoscale size and high concentration of defects in $Mg(BH_4)_2$ particles formed mechanochemically.

The dehydrogenated product was again hydrogenated by ball milling at $p_H$ = 350 bar, $\tau_{BM}$ = 15 h and B/S = 160. The $^{11}$B DPMAS spectrum of the re-hydrogenated sample (Fig. 4c) indicates that most of $MgB_2$ and polyhedral boron species were transformed back to $Mg(BH_4)_2$. Taken together, the spectra of Fig. 4a–c suggest a reasonable reversibility between $MgB_2$ and $Mg(BH_4)_2$. Compared to the first desorption, nearly 90% of the hydrogen desorption was recovered after the second mechanochemical hydrogenation cycle. The 10% loss of storage capacity may be attributed to the formation of elemental boron that remains unreacted in the rehydrogenated product, and in part to the additional Fe impurity introduced upon successive milling. Further cycling experiments have not been performed due to the difficulties in collecting the dehydrogenated product in quantities sufficient for adequate milling.

In summary, we have demonstrated purely mechanochemical hydrogenation of $MgB_2$ to $Mg(BH_4)_2$ by high energy reactive ball milling. The sample prepared at room temperature under 350 bar $H_2$ releases ~4 wt% of hydrogen below 390 °C. SSNMR reveals the formation of $Mg(BH_4)_2$ as the final product through $[B_xH_y]^{n-}$ intermediates. Subsequent thermal dehydrogenation results in complete decomposition of mechanochemically synthesized $Mg(BH_4)_2$ and $[B_xH_y]^{n-}$ anions, and the recovery of $MgB_2$ below 390 °C. The results suggest that the formation of nanoscale size particles plays a critical role for the reversible hydrogen storage in the $Mg(BH_4)_2$–$MgB_2$ system.

Research was supported by the U.S. Department of Energy, Office of Basic Energy Sciences, Division of Materials Sciences and Engineering under Contract No. DE-AC02-07CH11358. RD and IZ were supported by the US Civilian Research and Development Foundation (CRDF), Grant UKC2-2970-LV-09.

## Notes and references

1 B. Sakintuna, F. Lamari-Darkrim and M. Hirscher, *Int. J. Hydrogen Energy*, 2007, **32**, 1121.
2 H.-W. Li, S. Orimo, Y. Nakamori, K. Miwa, N. Ohba, S. Towata and A. Züttel, *J. Alloys Compd.*, 2007, **446**, 315.
3 Y. Nakamori, K. Miwa, A. Ninomiya, H. Li, N. Ohba, S. Towata, A. Züttel and S. Orimo, *Phys. Rev. B: Condens. Matter Mater. Phys.*, 2006, **74**, 045126.
4 H.-W. Li, K. Kikuchi, Y. Nakamori, N. Ohba, K. Miwa, S. Towata and S. Orimo, *Acta Mater.*, 2008, **56**, 1342.
5 G. L. Soloveichik, Y. Gao, J. Rijssenbeek, M. Andrus, S. Kniajanski, R. C. Bowman Jr., S.-J. Hwang and J.-C. Zhao, *Int. J. Hydrogen Energy*, 2009, **34**, 916.
6 G. Severa, E. Ronnebro and C. M. Jensen, *Chem. Commun.*, 2010, **46**, 421.
7 H.-W. Li, T. Matsunaga, Y. Yan, H. Maekawa, M. Ishikiriyama and S. Orimo, *J. Alloys Compd.*, 2010, **505**, 654.
8 (*a*) S. L. James, C. J. Adams, C. Bolm, D. Braga, P. Collier, T. Friscic, F. Grepioni, K. D. M. Harris, G. Hyett, W. Jones, A. Krebs, J. Mack, L. Maini, A. G. Orpen, I. P. Parkin, W. C. Shearouse, J. W. Steed and D. C. Waddell, *Chem. Soc. Rev.*, 2012, **41**, 413; (*b*) C. Suryanarayana, *Prog. Mater. Sci.*, 2001, **46**, 1; (*c*) V. P. Balema, in *Materials Challenges in Alternative and Renewable Energy Ceramic Transactions*, ed. G. Wicks, J. Simon, R. Zidan, E. Lara-Cursio, T. Adams, J. Zayas, A. Karkamkar, R. Sindelar and B. Garcia-Diaz, Amer. Ceramic Soc, Westerville, OH, 2011, vol. 224, p. 25.
9 T. Kobayashi, I. Z. Hlova, N. K. Singh, V. K. Pecharsky and M. Pruski, *Inorg. Chem.*, 2012, **51**, 4108.
10 D. Fenzke, D. Freude, T. Frohlich and J. Haase, *Chem. Phys. Lett.*, 1984, **111**, 171.
11 J. W. Wiench, V. P. Balema, V. K. Pecharsky and M. Pruski, *J. Solid State Chem.*, 2004, **177**, 648.
12 L. E. Drain, *Proc. Phys. Soc., London, Sect. A*, 1962, **80**, 1380.
13 J. C. C. Freitas, E. C. Passamani, M. T. D. Orlando, F. G. Emmerich, F. Garcia, L. C. Sampaio and T. J. Bonagamba, *Energy Fuels*, 2002, **16**, 1068.
14 Y. Yan, H.-W. Li, H. Maekawa, M. Aoki, T. Noritake, M. Matsumoto, K. Miwa, S. Towata and S. Orimo, *Mater. Trans., JIM*, 2011, **52**, 1443.
15 M. Chong, A. Karkamkar, T. Autrey, S. Orimo, S. Jalisatgi and C. M. Jensen, *Chem. Commun.*, 2011, **47**, 1330.
16 M. E. Jones and R. E. Marsh, *J. Am. Chem. Soc.*, 1954, **76**, 1434.
17 A. J. Du, S. C. Smith, X. D. Yao, C. H. Sun, L. Li and G. Q. Lu, *J. Nanosci. Nanotechnol.*, 2009, **9**, 4388.
18 Z. G. Zhang, F. P. Luo, H. Wang, J. W. Liu and M. Zhu, *Int. J. Hydrogen Energy*, 2012, **37**, 926.
19 J.-C. Zhao, D. A. Knight, G. M. Brown, C. Kim, S.-J. Hwang, J. W. Reiter, R. C. Bowman Jr., J. A. Zan and J. G. Kulleck, *J. Phys. Chem. C*, 2009, **113**, 2.



 